Structure and Properties of a Tetranuclear Iron(III) Cage Complex. A Model for Hemerythrin

Jonathan L. Sessler,* John W. Sibert, and Vincent Lynch

Department of Chemistry and Biochemistry, University of Texas at Austin, Austin, Texas 78712

John T. Markert* and Chris L. Wooten

Department of Physics, University of Texas at Austin, Austin, Texas 78712

Received June 22, 1992

The reaction of glutaric acid with LFe_2Cl_6 (L = 1,4–bis(1,4,7-triaza-1-cyclononyl)butane) in the presence of base and KPF_6 affords the novel tetranuclear cage complex $[LFe_2O(C_5H_6O_4)]_2(PF_6)_4$ (**2**). Complex **2** forms dichroic (orange and green) crystals in the triclinic space group $P\bar{1}$ (No. 2), with the following unit cell parameters: a = 11.141 (2) Å, b = 11.2344 (14) Å, c = 17.278 (2) Å, α = 72.648 (9)°, β = 74.477 (10)°, γ = 70.702 (10)°, V = 1913.5 (4) Å^3, and Z = 1. The structure of **2** contains two hemerythrin-like(μ-oxo)bis(μ-carboxylato)diiron(III) cores separated from one another by 7.748 (1) Å. Spectroscopic, magnetic, and electrochemical studies of **2** are presented and compared with those of the related tetranuclear complex $[LFe_2O(OAc)_2]_2(PF_6)_4$ (**1**). Both complexes **1** and **2** are shown to contain two magnetically-independent, antiferromagnetically-coupled diiron cores (**1**, J = −113 (2) cm^{-1}; **2**, J = −110 (2) cm^{-1}), which are retained in solution. The redox behavior of **2** differs substantially from that of **1** as determined by cyclic voltammetry. Reduction of **1** results in a cathodic peak at −620 mV versus Ag/AgCl for which there is no corresponding anodic peak. In **2**, however, there are two reduction peaks at −500 and −635 mV versus Ag/AgCl, respectively, which correspond, as seen in the reversed scan, to two oxidation peaks at −360 and −580 mV. This result indicates that the cage complex **2** is more stable to electrochemical reduction than complex **1**.

Introduction

The oxo-bridged binuclear iron(III) unit has been found at the active sites of a variety of proteins (e.g. hemerythrin, ribonucleotide reductase, purple acid phosphatase, methane monooxygenase, and rubrerythrin).[1] These proteins have been studied extensively by spectroscopic methods and, in two cases (hemerythrin and ribonucleotide reductase), have been characterized structurally by x-ray diffraction.[2,3] The wide variety of functions, coupled with a somewhat similar basic structural motif, has made this class of proteins a particularly attractive target for model studies.[4]

The most well-characterized of the non-heme, iron-containing proteins is the respiratory protein hemerythrin (Hr), in which the functional center contains a triply-bridged diiron unit.[1,5] In deoxyHr, two ferrous atoms are bridged by a hydroxo ligand and carboxylic acid residues from the side chains of glutamate and aspartate residues. Five imidazoles from histidine residues cap the diiron core leaving one of the iron atoms with a vacant coordination site for the binding of dioxygen. Dioxygen is bound end-on, as hydroperoxide, to form oxyHr.[6] OxyHr contains a binuclear oxo-bridged Fe(III) core in which the bridging carboxylates and capping imidazole ligands are retained. Other ligands, such as azide or thiocyanate, can replace the hydroperoxide to form metHr. In addition, there are two mixed-valence forms of the protein, semimet$_O$Hr and semimet$_R$Hr,[7] formed by one electron oxidation of deoxyHr and one electron reduction of metHr, respectively.

Since the independent syntheses of two (μ-oxo)bis (μ-carboxylato)diiron(III) complexes by Lippard[8] and Wieghardt[9] in 1983, there has been tremendous interest in the development of accurate model compounds for hemerythrin.[4] The existing hemerythrin (Hr) model complexes can be loosely categorized into two types. There are the structurally accurate models (i.e. those that contain a Hr-like $[Fe_2O(O_2CR)_2]$ core) and the functional models[10] (i.e. iron-containing complexes that react with dioxygen). As might be expected, the structural models far outnumber the functional models. In general, the structurally accurate Hr-model complexes suffer from being coordinatively saturated (no available sites for O_2 binding) and from an apparent instability with respect to changes in oxidation state. These two features are obviously essential for the success of a functional Hr model. One apparent exception to the latter case is the complex $[FeO(OAC)_2(MTACN)_2]^{2+}$, where MTACN = 1, 4, 7-trimethyl-1,4,7-triazacyclononane, which shows a quasi-reversible one-electron wave at −0.37 V versus SCE.[11] Converse to the structural models, the functional Hr models lack a structurally accurate, Hr-like diiron core and appear to bind oxygen as bridging peroxide. This contrasts with the end-on O_2 binding of the protein.

There, thus, remains a need for the development of model complexes containing the $[Fe_2O(O_2CR)_2]$ core that can attain

(1) Reviews: (a) Vincent, J. B.; Olivier-Lilley, G. L.; Averill, B. A. *Chem. Rev.* **1990**, *90*, 1447–1467. (b) Que, L., Jr.; Scarrow, R. C. In *Metal Clusters in Proteins*; Que, L., Jr., Ed.; ACS Symposium Series 372 American Chemical Society: Washington, DC, 1988; pp 152–178. (c) Lippard, S. J. *Angew. Chem., Int. Ed. Engl.* **1988**, *27*, 344–361.
(2) (a) Stenkamp, R. E.; Sieker, L. C.; Jensen, L. H. *J. Am. Chem. Soc.* **1984**, *106*, 618–622. (b) Sheriff, S.; Hendrickson, W. A.; Smith, J. L. *J. Mol. Biol.* **1987**, *197*, 273–296 and references therein.
(3) Norlund, P.; Sjöberg, B.-M.; Eklund, H. *Nature (London)* **1990**, *345*, 593–598.
(4) Review: Kurtz, D. M., Jr. *Chem. Rev.* **1990**, *90*, 585–606.
(5) (a) Wilkins, R. G.; Harrington, P. C. *Adv. Inorg. Biochem.* **1983**, *5*, 51–85. (b) Klotz, I. M.; Kurtz, D. M., Jr. *Acc. Chem. Res.* **1984**, *17*, 16–22.
(6) Shiemke, A. K.; Loehr, T. M.; Sanders-Loehr, J. *J. Am. Chem. Soc.* **1986**, *108*, 2437–2443.
(7) McCormick, J. M.; Solomon, E. I. *J. Am. Chem. Soc.* **1990**, *112*, 2005–2007 and references therein.
(8) Armstrong, W. H.; Lippard, S. J. *J. Am. Chem. Soc.* **1983**, *105*, 4837–4838.
(9) Wieghardt, K.; Pohl, K.; Gebert, W. *Angew. Chem.* **1983**, *95*, 739–740.
(10) (a) Menage, S.; Brennan, B. A.; Juarez-Garcia, C.; Münck, E.; Que, L., Jr. *J. Am. Chem. Soc.* **1990**, *112*, 6423–6425. (b) Kitajima, N.; Fukui, H.; Moro-oka, Y. *J. Am. Chem. Soc.* **1990**, *112*, 6402–6403. (c) Tolman, W. B.; Bino, A.; Lippard, S. J. *J. Am. Chem. Soc.* **1989**, *111*, 8522–8523.
(11) Hartman, J. R.; Rardin, R. L.; Chaudhuri, P.; Pohl, K.; Wieghardt, K.; Nuber, B.; Weiss, J.; Papaefthymiou, G. C.; Frankel, R. B.; Lippard, S. J. *J. Am. Chem. Soc.* **1987**, *109*, 7387–7396.

0020-1669/93/1332-0621$04.00/0

other oxidation states and that have a vacant coordination site for the binding of small anions and, ultimately, dioxygen. It is the former criterion that we wish to address in this work. Through the development and study of functionally and structurally accurate model compounds we hope to gain insight into how a common structure, the oxo-bridged diiron unit, can perform such a wide variety of functions in biology.

We recently described the synthesis of the ligand 1,4-bis(1,4,7-triaza-1-cyclononyl)butane, L, as well as the tetranuclear iron(III) hemerythrin model complex $[LFe_2O(O_2CCH_3)_2]_2(PF_6)_4$ (**1**),

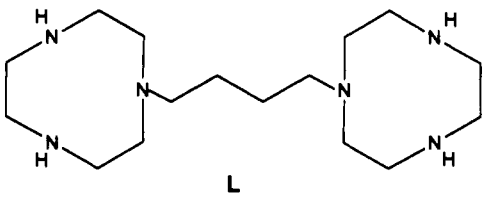

L

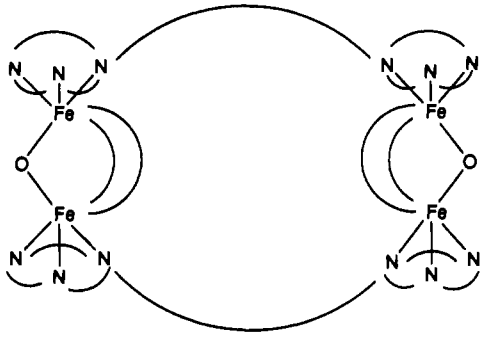

$[LFe_2O(O_2CCH_3)_2]_2^{4+}$ (1)

which it stabilizes.[12] Complex **1**, containing two distinct (μ-oxo)bis(μ-acetato)diiron(III) cores, was shown to mimic successfully the essential structural and spectroscopic features of metazidohemerythrin. In an effort to increase the rigidity of complex **1** and, perhaps, the stability, we sought to prepare a tetrameric complex analogous to **1** in which the two diiron cores are further linked through their respective bridging carboxylate ligands. We now wish to report the synthesis and structural characterization of such a system, namely the title complex $[LFe_2O(C_5H_6O_4)]_2(PF_6)_4$ (**2**), in which two $[Fe_2O(O_2CR)_2]^{2+}$ cores are linked by both the capping ligands L and by two glutarate dianions. In addition, we present here a comparative study of the magnetic and electrochemical behavior of complexes **1** and **2**.

Experimental Section

Materials and Apparatus. The ligand 1,4-bis(1,4,7-triaza-1-cyclononyl)butane, L, and the complex LFe_2Cl_6 were prepared as described previously.[12] Glutaric acid was obtained from Aldrich Chemical Co. All other reagents and solvents were of reagent grade quality, obtained from commercial suppliers, and used without further purification. Electronic spectra were recorded on a Beckman DU-7 spectrophotometer. Fourier transform infrared spectra were obtained on a Bio-Rad FTS-40 spectrophotometer. Elemental analysis was performed by Atlantic Microlab.

Preparation of $[LFe_2(\mu\text{-}O)(C_5H_6O_4)]_2(PF_6)_4$ (2). To a suspension of LFe_2Cl_6 (240 mg) in ethanol (75 mL) was added glutaric acid (50.0 mg) and excess triethylamine (1–2 mL). The solution rapidly turned a deep orange-brown color. After the solution was stirred for 6 h, an excess of KPF_6 (250 mg) was added. The solvent was then removed on a rotary evaporator. The residue was taken up in acetone, and a white solid, presumably NaCl and KCl, was filtered away. The acetone was removed by evaporation to leave an orange-brown solid. Pure **2** was obtained as orange-brown crystals by vapor diffusion of methanol into an acetonitrile solution containing **2**. For analysis, this sample was further subject to extensive drying in vacuo. For the X-ray analysis, diffraction-quality dichroic (green and orange) crystals were grown by the vapor diffusion of ether into an acetonitrile solution of **2** at 5 °C. IR (KBr, cm^{-1}, selected peaks): 3331 (s), 2950 (m), 1558 (s), 1458 (m), 1446 (m), 1419 (s), 842 (vs), 733 (m), 558 (s). UV–vis [λm nm (ϵ, M^{-1} cm^{-1}/Fe)]: 340 (3715), 422 (451), 471 (653), 513 (475), 552 (102), 731 (63). Anal. Calcd for $C_{42}H_{84}N_{12}O_{10}Fe_4P_4F_{24}$: C, 29.30; H, 4.92; N, 9.77. Found: C, 28.84; H, 4.81; N, 9.55. Complex **2** was further characterized by X-ray crystallography.

Table I. Crystallographic Data for **2**

chem formula	$C_{50}H_{96}N_{16}O_{10}P_4F_{24}Fe_4$	space group	$P\bar{1}$ (No. 2)
		T, °C	−75
a, Å	11.141 (2)	λ(Mo Kα), Å	0.7107
b, Å	11.2344 (14)	ρ_{calc}, g/cm^3 (−75 °C)	1.64
c, Å	17.278 (2)	no. of reflcns measd	9298
α, deg	72.648 (9)	no. of unique reflcns	8845
β, deg	74.477 (10)	R_{int}	0.011
γ, deg	70.702 (10)	μ, cm^{-1}	9.412
V, Å^3	1913.5 (4)	transm coeff	0.6336–0.8655
Z	1	$R(F)$	0.0358
fw	1884.65	$R_w(F)$	0.0433
cryst system	triclinic		

X-ray Crystallography. The data crystal was a plate of approximate dimensions 0.16 × 0.48 × 0.48 mm. The crystal was orange as viewed by transmitted light through the thin section (0.16 mm) of the plate which corresponds to (001). The data were collected at −75 °C on a Nicolet R3 diffractometer, with a graphite monochromator using Mo Kα radiation (λ = 0.7107 Å) and equipped with a Nicolet LT-2 low-temperature delivery system. Details of crystal data and refinement are listed in Table I. The lattice parameters were obtained from least-squares refinement of 50 reflections with $20.2 < 2\theta < 25.5°$. The data were collected using the ω-scan technique from 4 to 55° in 2θ, with a scan width of 1.2° and a scan rate of 3–6°/min. A total of 9298 reflections were collected, of which 8845 were unique (h ranged from 0 to 13; k from −13 to 13; l from −21 to 21). The R for averaging equivalent reflections was 0.011. Four reflections (−3,−4,−8; −3,1,6; 3,−3,3; 3,5,0) were remeasured every 96 reflections to monitor instrument and crystal stability. A smoothed curve of the intensities of these check reflections was used to scale the data. The scaling factor ranged from 0.905 to 1.06. The data were also corrected for Lp effects and absorption (based on crystal shape measurements). Reflections having $F_o < 4(\sigma(F_o))$ were considered unobserved (1822 reflections). The structure was solved by direct methods and refined by full-matrix least-squares procedures with anisotropic thermal parameters for the non-hydrogen atoms. The methyl hydrogens on the acetonitrile C's were calculated in idealized positions (C–H = 0.96 Å), while all other hydrogen atoms were located from a difference electron density map. All hydrogens were refined with isotropic thermal parameters except for the idealized methyl hydrogen atoms which were fixed at $1.2U_{eq}$ of the relevant C. A total of 655 independent parameters were refined. The data were checked for secondary extinction errors which were found to be insignificant. The function $\Sigma w(|F_o| - |F_c|)^2$ was minimized, where $w = 1/(\sigma(F_o))^2$ and $\sigma(F_o) = 0.5kI^{-1/2}[(\sigma(I))^2 + (0.02I)^2]^{1/2}$. The intensity, I, is given by $(I_{peak} = I_{bkgd}) \times$ (scan rate), 0.02 is a factor to downweight intense reflections and to account for instrument instability, and k is the correction due to Lp effects, absorption, and decay. $\sigma(I)$ was estimated from counting statistics; $\sigma(I) = [(I_{peak} + I_{bkgd})^{1/2} \times$ (scan rate)]. Final R = 0.0358 for 7023 reflections, R_w = 0.0433 (R for all reflections = 0.0491, R_w for all reflections = 0.0455), and the goodness of fit = 1.507. The maximum |shift/esd| < 0.1 in the final refinement cycle, and the minimum and maximum peaks in the final difference electron density map were −0.37 and 0.48 e/Å^3, respectively. The structure solution and refinement were done using SHELXTL-PLUS.[13] The scattering factors for the non-H atoms were taken from Cromer and Mann,[14] with anomalous-dispersion corrections from Cromer and Liberman,[15] while scattering factors for the H atoms were obtained from Stewart, Davidson, and Simpson.[16] The linear absorption coefficient was calculated from values in ref 17. Other computer programs were

(12) Sessler, J. L.; Sibert, J. W.; Lynch, V. *Inorg. Chem.* **1990**, *29*, 4143–4146.

(13) SHELXTL-PLUS; Nicolet Instrument Corp.: Madison, WI, 1987.
(14) Cromer, D. T.; Mann, J. B. *Acta Crystallogr.* **1968**, *A24*, 321–324.
(15) Cromer, D. T.; Liberman, D. *J. Chem. Phys.* **1970**, *53*, 1891–1898.
(16) Stewart, R. F.; Davidson, E. R.; Simpson, W. T. *J. Chem. Phys.* **1965**, *42*, 3175–3187.
(17) *International Tables for X-ray Crystallography*; Kynoch: Birmingham, England, 1974; Vol. IV, p 55.

Table II. Fractional Coordinates and Equivalent Isotropic Thermal Parameters (Å²) for the Non-Hydrogen Atoms of **2**

atom	x	y	z	U^a
Fe1	0.48257 (3)	0.71975 (3)	0.71112 (2)	0.01820 (12)
Fe2	0.20749 (3)	0.90265 (3)	0.70625 (2)	0.01821 (11)
N1	0.6998 (2)	0.6287 (2)	0.66841 (11)	0.0208 (7)
C2	0.7007 (2)	0.5052 (2)	0.65327 (15)	0.0259 (9)
C3	0.6235 (3)	0.4304 (2)	0.7258 (2)	0.0304 (10)
N4	0.4973 (2)	0.5166 (2)	0.75687 (13)	0.0257 (8)
C5	0.4628 (3)	0.5003 (3)	0.8481 (2)	0.0320 (10)
C6	0.5456 (3)	0.5570 (3)	0.87658 (15)	0.0314 (10)
N7	0.5566 (2)	0.6843 (2)	0.82106 (12)	0.0246 (7)
C8	0.6910 (2)	0.6959 (3)	0.79494 (15)	0.0278 (9)
C9	0.7689 (2)	0.6080 (2)	0.73637 (15)	0.0253 (9)
C10	0.7553 (2)	0.7123 (2)	0.59119 (14)	0.0215 (8)
C11	0.8891 (2)	0.6471 (2)	0.54691 (15)	0.0254 (9)
C12	0.9600 (2)	0.7444 (2)	0.48777 (15)	0.0250 (8)
C13	0.8774 (2)	0.8416 (2)	0.42624 (14)	0.0220 (8)
N14	0.9446 (2)	0.9261 (2)	0.35540 (11)	0.0198 (7)
C15	1.0291 (2)	0.8516 (2)	0.29243 (15)	0.0258 (9)
C16	0.9631 (3)	0.8801 (2)	0.22004 (15)	0.0266 (9)
N17	0.9127 (2)	1.0221 (2)	0.19004 (12)	0.0237 (7)
C18	1.0151 (2)	1.0903 (3)	0.14789 (15)	0.0285 (9)
C19	0.9872 (3)	1.2120 (3)	0.17856 (15)	0.0299 (10)
N20	0.9489 (2)	1.1824 (2)	0.26989 (12)	0.0236 (7)
C21	1.0555 (2)	1.1000 (3)	0.3146 (2)	0.0279 (10)
C22	1.0152 (2)	0.9908 (3)	0.38333 (15)	0.0258 (9)
O23	0.31504 (14)	0.76338 (14)	0.75774 (9)	0.0216 (6)
O24	0.51839 (14)	0.89778 (15)	0.66465 (10)	0.0241 (6)
O25	0.31519 (15)	1.02586 (15)	0.68071 (10)	0.0251 (6)
C26	0.4352 (2)	1.0070 (2)	0.65287 (13)	0.0202 (8)
C27	0.4757 (2)	1.1230 (3)	0.5974 (2)	0.0354 (10)
C28	0.6142 (2)	1.1265 (2)	0.58610 (14)	0.0246 (9)
C29	0.6397 (2)	1.2435 (2)	0.51694 (14)	0.0231 (9)
C30	0.6377 (2)	1.2229 (2)	0.43514 (13)	0.0191 (8)
O31	0.73311 (15)	1.1378 (2)	0.40741 (10)	0.0260 (6)
O32	0.53999 (15)	1.28426 (15)	0.40150 (9)	0.0234 (6)
P1	0.21207 (7)	0.45879 (6)	0.67702 (4)	0.0319 (3)
F1	0.3548 (2)	0.4712 (3)	0.64224 (14)	0.0733 (11)
F2	0.2082 (2)	0.5095 (2)	0.75515 (12)	0.0666 (10)
F3	0.1536 (2)	0.6042 (2)	0.62972 (12)	0.0640 (9)
F4	0.2195 (2)	0.4105 (2)	0.59866 (13)	0.0667 (10)
F5	0.2672 (2)	0.3153 (2)	0.72652 (13)	0.0621 (9)
F6	0.0705 (2)	0.4447 (2)	0.71273 (15)	0.0767 (11)
P2	0.27474 (7)	0.82756 (8)	0.00270 (4)	0.0365 (3)
F7	0.2612 (2)	0.7129 (2)	−0.02718 (15)	0.0718 (11)
F8	0.4256 (2)	0.7594 (2)	−0.00113 (3)	0.0671 (10)
F9	0.3062 (2)	0.9004 (2)	−0.09205 (10)	0.0602 (9)
F10	0.1243 (2)	0.8950 (2)	0.00600 (12)	0.0595 (9)
F11	0.2456 (2)	0.7527 (2)	0.09616 (12)	0.0734 (10)
F12	0.2883 (2)	0.9434 (2)	0.03083 (12)	0.0638 (10)
N33	0.3503 (4)	0.9497 (5)	0.2089 (2)	0.098 (2)
C34	0.4430 (3)	0.9104 (4)	0.1683 (2)	0.054 (2)
C35	0.5642 (4)	0.8572 (4)	0.1169 (2)	0.064 (2)
N36	0.8101 (5)	0.6207 (6)	−0.0040 (3)	0.118 (3)
C37	0.8743 (5)	0.6384 (5)	0.0309 (3)	0.090 (3)
C38	0.9570 (6)	0.6589 (7)	0.0735 (3)	0.124 (4)

[a] For anisotropic atoms, the U value is U_{eq}, calculated as $U_{eq} = {}^1/_3\sum_i\sum_j U_{ij}a_i^*a_j^*A_{ij}$, where A_{ij} is the dot product of the ith and jth direct space unit cell vectors.

from ref 11 of Gadol and Davis.[18] Fractional coordinates and U values are found in Table II.

Magnetic Susceptibility Measurements. Solid-state magnetic susceptibilities of powdered samples of **1** and **2** were measured between 2 and 300 K at a field of 10 kG using a Quantum Design Model MPMS SQUID magnetometer. Totals of 74 data points for **1** and 70 data points for **2** were measured. The susceptibilities were corrected for the magnetism of the quartz sample holder. Gram susceptibilities were then converted to molar susceptibilities. Diamagnetic corrections were calculated for **1** (-844×10^{-6} cgs/mol) and **2** (-856×10^{-6} cgs/mol) using Pascal's constants.[19]

A model to describe the magnetic behavior of both **1** and **2** is based on the two diiron(III) core units in the tetranuclear iron complex behaving as discrete magnetic entities. In this case, the molar paramagnetic susceptibility data are fit to an expression, derived elsewhere,[20] which is based on the general isotropic exchange Hamiltonian, $H = -2JS_1 \cdot S_2$, with J = magnetic exchange coupling constant and $S_1 = S_2 = {}^5/_2$:

$$\chi_M^{corr} = \frac{(1-p)C(2e^{2x} + 10e^{6x} + 28e^{12x} + 60e^{20x} + 110e^{30x})}{1 + 3e^{2x} + 5e^{6x} + 7e^{12x} + 9e^{20x} + 11e^{30x}} + \frac{4.375p}{T} + \text{TIP} \quad (1)$$

Here $C = N_g^2\mu_B^2/kT$, $x = J/kT$, and p = mole percentage of paramagnetic impurity. The temperature-independent paramagnetic susceptibility term (TIP) results from the mixing of nonthermally populated wave functions of low-lying excited states into the ground-state wave function. For our purposes, this term was excluded because the ground state of high-spin iron(III) is much lower in energy than its first excited state.[21] The $4.375/T$ term accounts for the spin-only magnetism associated with a paramagnetic iron(III) ($S = {}^5/_2$) impurity of mole percentage "p". The value of g was fixed at 2.0 for all fits.

Solution magnetic susceptibilities were determined in CD_3CN by ^1H NMR using the Evans method.[22,23] A value of -0.5×10^{-6} cgs/g was used for the mass susceptibility of acetonitrile.[24] Diamagnetic corrections for **1** and **2** were used as stated above. The corrected molar susceptibilities were then converted to magnetic moments per Fe using a suitable form of Curie's Law, $\mu_{eff} = 2.84[(\chi_M^{corr})/4 \cdot T]^{1/2}$. Spectra were recorded on a General Electric QE-300 (300 MHz) spectrometer.

Electrochemistry. Cyclic voltammetry measurements for **1** and **2** were performed at room temperature under an argon atmosphere with a conventional three-electrode system. A platinum working electrode was subjected to a series of background scans to establish a stable baseline prior to each series of measurements. A platinum wire was used as a counter electrode. A Ag/AgCl electrode was used as the reference electrode and was separated from the bulk solution by a fritted glass bridge which contained CH_3CN and the supporting electrolyte, 0.1 M tetra-*n*-butylammonium/perchlorate (TBAP). Ferrocene was used as an internal calibrant ($E_{1/2} = 422$ mV; $\Delta E_{pp} = 65$ mV). A Pine Instruments Co. Model RDE-4 potentiostat/galvanostat was used to control the potential. Current–voltage curves were recorded on a Kipp & Zonen Model BD-90 recorder.

Results and Discussion

We have explored the iron(III) coordination chemistry of 1,4-bis(1,4,7-triaza-1-cyclononyl)butane, L, to model the active sites of iron–oxo proteins. We have previously reported the reaction of L with 2 equiv of $FeCl_3 \cdot 6H_2O$ in ethanol to produce the yellow binuclear complex LFe_2Cl_6.[12] Following treatment with a source of acetate, the tetrameric Hr-model complex $[LFe_2O(O_2CCH_3)_2]_2(PF_6)_4$ (**1**) was obtained. In an effort to enhance the rigidity, and, perhaps, the stability of this tetrameric model complex to electrochemical reduction, we sought to synthesize a tetranuclear iron(III) complex in which the four acetate ligands are replaced by two dicarboxylic acids of a suitable length. It was our premise that the dicarboxylic acids would serve to help keep the complex intact upon changes in oxidation state. It was determined from the X-ray structure of **1** and with the aid of CPK models that a dicarboxylic containing four or five carbon atoms (e.g. succinate or glutarate) would provide the proper length to span the two diiron cores.

The desired cage complex, **2**, readily self-assembles upon the addition of 1 equiv of glutaric acid to LFe_2Cl_6 in the presence of triethylamine. Interestingly, as shown in Table III, complexes **1** and **2** have nearly identical electronic and vibrational spectra. This not only indicates the presence of a (μ-oxo)bis(μ-carboxylato)diiron(III) core in **2** but suggests a strong structural correlation between the two complexes. Following metathesis with PF_6^-, single, X-ray quality, dichroic (green and orange) crystals of **2** were obtained and subjected to X-ray diffraction analysis.

(18) Gadol, S. M.; Davis, R. E. *Organometallics* **1982**, *1*, 1607–1613.
(19) Carlin, R. L. In *Magnetochemistry*; Springer-Verlag: Berlin, 1986; p 3.
(20) O'Connor, C. J. *Prog. Inorg. Chem.* **1982**, *29*, 203–283.
(21) Carlin, R. L. In *Magnetochemistry*; Springer-Verlag: Berlin, 1986, 64.
(22) Evans, D. F. *J. Chem. Soc.* **1959**, 2003–2005.
(23) Armstrong, W. H.; Spool, A.; Papaefthymiou, G. C.; Frankel, R. B.; Lippard, S. J. *J. Am. Chem. Soc.* **1984**, *106*, 3653–3667.
(24) Bailey, R. A. *J. Chem. Educ.* **1972**, *49*, 297–299.

Table III. Structural (Å, deg) and Spectroscopic Data for Complexes **1** and **2** and Azidometmyohemerythrin

	1	2	azidometmyohemerythrin
Fe–O	1.793 (3); 1.794 (3)	1.788 (1); 1.782 (1)	1.77; 1.80
Fe–O, carboxylate (av)	2.014 (2)	2.032 (1)	2.10
Fe–N, cis (av)	2.158 (2)	2.145 (1)	2.13
Fe–N, trans	2.286 (3)	2.302 (1)	2.24
Fe···Fe, within core	3.087 (1)	3.081 (1)	3.23
Fe···Fe, between cores[a]	7.785 (1); 7.929 (9)[b]	7.748 (1)	
Fe–O–Fe	119.84 (14)	119.29 (8)	130
λ_{max}, nm[c]	739 (111)	731 (63)	680 (95)
(ϵ, cm^{-1} (mol of Fe)$^{-1}$ L)	551 (sh)	552 (102)	
	513 (563)	513 (475)	
	471 (745)	471 (653)	446 (1850)
	423 (sh)	422 (451)	
	338 (3818)	340 (3715)	326 (3375)
ν_{asym}(Fe–O–Fe), cm^{-1}	732	733	770
$\nu_{sym}(CO_2)$, cm^{-1}	1430, 1452	1419, 1446, 1458	
$\nu_{asym}(CO_2)$, cm^{-1}	1556	1558	
J, cm^{-1}	−113 (2)	−110 (2)	−134
ref	12, this work	this work	2b, 23, 30

[a] Center to center distance (equal to Fe1–Fe2'). [b] Two similar tetrameric structures have been characterized for complex **1**. The only structural difference between the two complexes is the distance between the two diiron cores. [c] Solvent for **1** and **2** is acetonitrile.

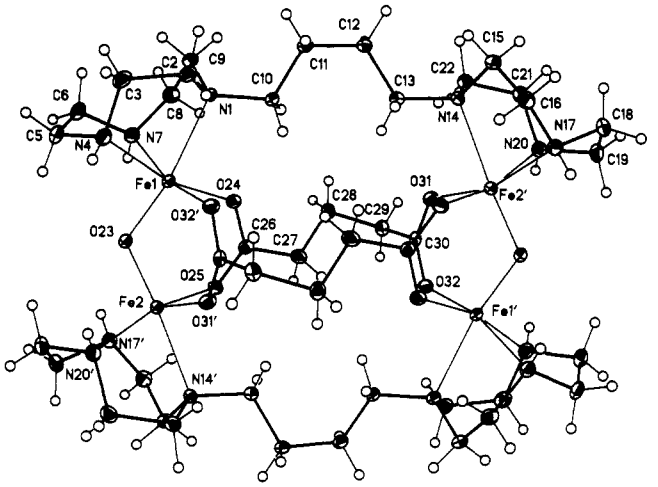

Figure 1. View of **2**, showing the atom labeling scheme. Thermal ellipsoids are scaled to the 30% probability level. H atoms are drawn to an arbitrary size. The complex lies around an inversion center. Atoms labeled by primes are related by $1-x, 2-y, 1-z$. The coordination around the Fe atoms is pseudo-octahedral with the Fe's lying slightly out of the equatorial plane of two N and two carboxylate O donors and directed toward the μ-oxo O. The axial N–Fe bonds (2.302 (1) Å average) are longer than the equatorial N–Fe bonds (2.145 (1) Å average) presumably due to a trans-effect by the μ-oxo O.

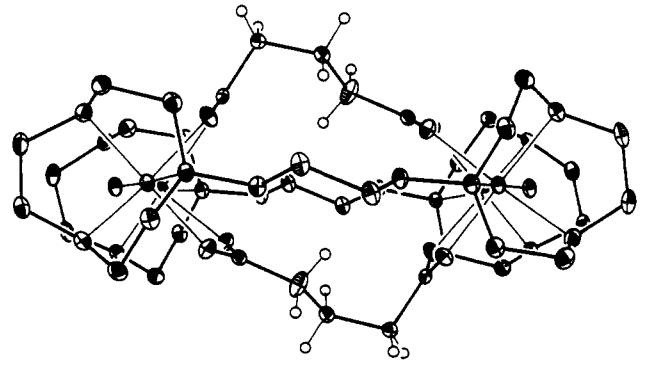

Figure 2. View of the cation of **2** looking along the Fe–O–Fe plane and illustrating the conformation of the hydrocarbon tethers and the glutarate linkages. Most of the H atoms have been removed for clarity.

Description of the Structure. As shown in Figures 1 and 2, **2** is a tetranuclear iron(III) complex, composed of two (μ-oxo)bis(μ-carboxylato)diiron cores. The "dimer of dimers" structure exhibited by **2** is similar to that for the acetate-bridged system **1** and also for two other tetranuclear iron(III) hemerythrin model complexes in the literature.[25] We also note that Wieghardt et al., in the absence of an X-ray structural determination, reported stabilization of a dinuclear iron(III) Hr-model complex from the ligand 1,2-bis(1,4,7-triaza-1-cyclononyl)ethane.[26] However, in light of the structurally characterized tetranuclear complexes described above, Wieghardt's complex probably also contains the "dimer of dimers" structure and is, thus, more aptly described as being tetranuclear.[12,25a] Interestingly, all of these tetranuclear complexes have one common structural element: The ligands used to cap the diiron(III) cores contain two distinct binding sites that are linked through a noninteracting hydrocarbon tether (i.e. there is no ligating functionality, such as phenoxide or alkoxide, on the tether). This type of ligand system uniquely appears to promote tetranuclear, and not binuclear, complex formation. It is our premise then that the hydrocarbon tether of, for example ligand L in complexes **1** and **2**, prevents, probably by a steric interaction with the metal-to-metal bridges, the formation of dimeric Hr-model complexes. This steric interaction is relieved by tetramer formation.

Complex **2** lies around an inversion center. Each iron atom is in an approximately octahedral coordination environment with the outer faces of the diiron core capped by TACN (1,4,7-triazacyclononane) macrocycles from ligand L. The two dinuclear cores are linked not only by the butylene bridge of L but also by two glutarate ligands. The bridging mode of the glutarate ligand in **2** is quite different from that of several other recently reported Hr-model complexes containing the dicarboxylate ligand *m*-phenylenedipropionate (MPDP).[27] In these complexes, the MPDP ligand provides both bridging carboxylates to one diiron(III) core, while, in **2**, the glutarate ligand spans two distinct diiron(III) cores.

Structurally, complexes **1** and **2** and azidometHr are very similar (see Table III). As in complex **1**, there is a trans influence exhibited by the oxo bridge in **2** which results in the lengthening of the Fe–N_{trans} bond (2.302 (1) Å) relative to the two Fe–N_{cis} bonds (average = 2.145 (1) Å). This feature is characteristic of the (μ-oxo)bis(μ-carboxylato)diiron(III) core and is found in other model complexes as well as azidometHr, itself.[1,4] The Fe···Fe distances within each diiron core (**1**, 3.087 (1) Å; **2**, 3.081 (1) Å) and between the cores (**1**, average = 7.859 (1) Å; **2**, 7.748 (1) Å) are similar in both **1** and **2**. The average Fe–O(glutarate)

(25) (a) Toftlund, H.; Murray, K. S.; Zwack, P. R.; Taylor, L. F.; Anderson, O. P. *J. Chem. Soc., Chem. Commun.* **1986**, 191–193. (b) Sessler, J. L.; Hugdahl, J. D.; Lynch, V.; Davis, B. *Inorg. Chem.* **1991**, *30*, 334–336.
(26) Wieghardt, K.; Tolksdorf, I.; Herrmann, W. *Inorg. Chem.* **1985**, *24*, 1230–1235.
(27) Beer, R. H.; Tolman, W. B.; Bott, S. G.; Lippard, S. *J. Inorg. Chem.* **1991**, *30*, 2082–2092.

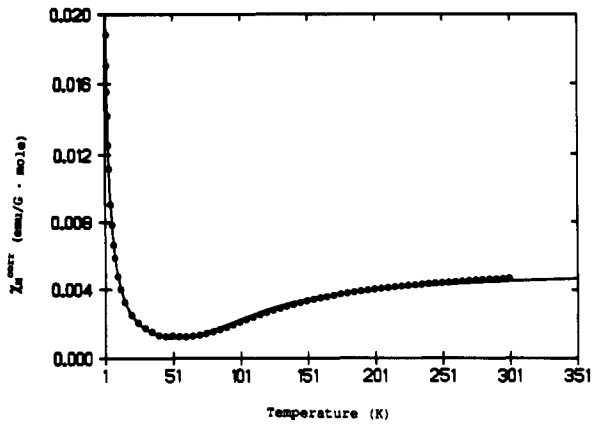

Figure 3. Plot of χ_M^{corr} (●) vs T for solid **2**. The line represents the best least-squares fit of eq 1 (see text) to the experimental susceptibility data.

bond length (2.032 (1) Å) is typical for Fe–O(carboxylate) bonds.[8,9,12,23,25,27] The Fe–O–Fe bridge is symmetrical in both **1** and **2** (Fe–O = 1.793 (3) Å for Fe1 and 1.794 (3) Å for Fe2 and Fe–O–Fe = 118.78 (14)° for **1**; Fe–O = 1.788 (2) Å for Fe1 and 1.782 (1) Å for Fe2 and Fe–O–Fe = 119.28 (8)° for **2**).[28]

Magnetic Susceptibility. A nonlinear least-squares fitting program[29] was used to fit the observed variable temperature magnetic susceptibility data for **1** and **2** to eq 1. With g fixed at 2.0, optimization of the data fit for **2** gave $J = -110$ (2) cm^{-1} and $p = 1.10 \times 10^{-2}$ with a correlation coefficient of 0.9990 (Figure 3). In the case of complex **1**, the best fit with g fixed at 2.0 gave $J = -113$ (2) cm^{-1} and $p = 7.76 \times 10^{-3}$ with a correlation coefficient of 0.9956. The large negative value for J demonstrates that the two iron atoms within each of the diiron cores in **1** and **2** are strongly antiferromagnetically coupled. Furthermore, the excellent fit of both sets of data to eq 1 indicates that our assumption of the two diiron cores in both **1** and **2** behaving as independent magnetic entities is a valid one. This seems reasonable as the π-mediated superexchange pathway (Fe–O–Fe) within each diiron core is expected to dominate over any coupling of the two diiron cores through space (as in **1**) or by the longer range σ-bond pathway of the glutarate ligand (as in **2**).

The J values for **1** and **2** are somewhat less than that found for the met form of Hr isolated from *Golfingia gouldii* ($J = -134$ cm^{-1}).[30] In addition, they are slightly smaller than those reported for other bi- and tetranuclear iron(III) Hr-model complexes, which have J values that typically range from -115 to -124 cm^{-1}.[4] These slightly smaller J values are not interpreted as a significantly weaker antiferromagnetic coupling interaction in complexes **1** and **2** as compared to the other Hr-model complexes. Instead, we note that Kurtz has suggested as much as a 10% difference in J values reported from separate laboratories due just to the different methods used in obtaining fits.[4] The antiferromagnetic interactions in **1** and **2** are, thus, not anomalous but considered consistent with those in related complexes.[31]

The molar susceptibilities of **1** and **2** were determined in acetonitrile using the Evan's NMR method.[22] This technique has been used to demonstrate the integrity of the (μ-oxo)bis(μ-carboxylato)diiron(III) core in solution.[4] Two room-temperature trials for **1** gave values for χ_M^{corr} of 4.41×10^{-3} and 4.92×10^{-3} cgs/mol. A μ_{eff} was then calculated from Curie's Law and found to be equal to 1.63 μ_B and 1.72 μ_B, respectively. These magnetic moments are in excellent agreement with the room-temperature magnetic moment for **1** in the solid state ($\mu_{eff} = 1.64$ μ_B; $\chi_M^{corr} = 4.45 \times 10^{-3}$ cgs/mol) as determined from the SQUID magnetometry data. In the case of **2**, the room-temperature magnetic moment in solution ($\mu_{eff} = 1.73$ μ_B; $\chi_M^{corr} = 4.99 \times 10^{-3}$ cgs/mol) also agrees well with that obtained in the solid state ($\mu_{eff} = 1.68$ μ_B; $\chi_M^{corr} = 4.66 \times 10^{-3}$ cgs/mol). This confirms the presence of the (μ-oxo)bis(μ-carboxylato)diiron(III) core in solution for both complexes **1** and **2**.

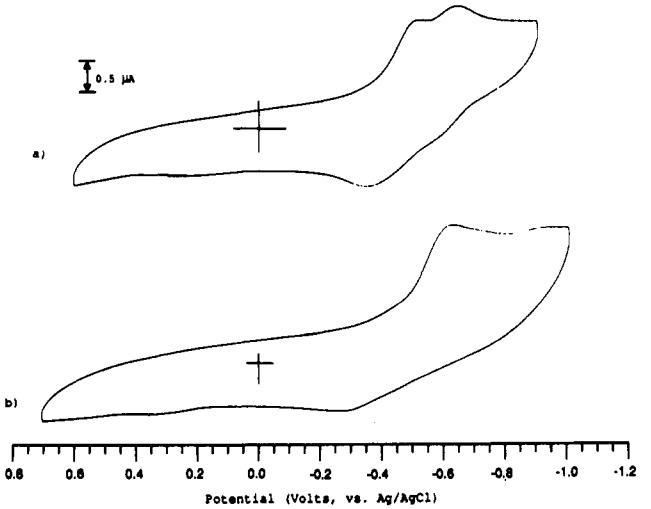

Figure 4. Cyclic voltammogram of (a) **2** at 200 mV/s scan speed in acetonitrile containing 0.1 M tetra-*n*-butylammonium perchlorate and (b) **1** at 200 mV/s scan speed in acetonitrile containing 0.1 M tetra-*n*-butylammonium perchlorate.

Unfortunately, these results provide little information as to the nuclearity of complexes **1** and **2** in solution. In general, the nature of the capping ligand does not dramatically affect the degree of antiferromagnetic coupling in complexes containing the $[Fe_2O(O_2CR)]^{2+}$ core. As a consequence, if the solid-state tetrameric structures of **1** and **2** persist in solution, they would very possibly have indistinguishable magnetic properties from putative dimeric or, perhaps, even higher order oligomeric structures. We, therefore, cannot rule out the presence of other oligomeric species (in particular, dimers) containing the (μ-oxo)-bis(μ-carboxylato)diiron(III) core in solutions of either **1** or **2**.

Electrochemical Studies. The electrochemical behavior of **1** and **2** has been studied using cyclic voltammetry. During the cathodic sweep of complex **1**, a reduction wave is seen at –620 mV (vs Ag/AgCl) for which there appears to be no corresponding oxidation wave (see Figure 4, voltammogram "b"). Increasing the scan rate to 800 mV/s still fails to produce any coupled oxidation wave indicating that the reduction is completely irreversible. Two small inflections can be seen at –290 and 300 mV on the return scan. A similar instability with respect to electrochemical reduction was observed in $[Fe_2O(O_2CCH_3)_2\{HB(pz)_3\}_2]$ ($HB(pz)_3$ = hydrotris(1-pyrazolyl)borate),[23] for which an irreversible reduction occurred at –760 mV (vs SCE), and in $[Fe_2O(MPDP)\{HB(pz)_3\}_2]$, for which an irreversible reduction occurred at –895 mV (vs Ag/AgCl).[27] The latter complex, containing the dicarboxylate *m*-phenylenedipropionate, demonstrates that linking the two carboxylates in *one* $[Fe_2O(O_2CR)_2]^{2+}$ core does not prevent reductive decomposition.

The electrochemical behavior of **2** differs considerably from that of **1** (see Figure 4). At a potential scan rate of 200 mV/s, the current/potential profile for **2** shows two consecutive peaks in reduction at –500 mV (vs Ag/AgCl) and –635 mV, respectively, followed, in the reversed scan, by an inflection at –580 mV and an oxidation peak at –360 mV. The peaks do not significantly shift on the potential axis as a function of scan rate (measured

(28) In the original report,[12] an error was made in inputting the value of the *b* axis for structure **1** (as 22.352 instead of 23.352). This error results in slight but significant differences in the calculated values of some bond lengths and angles. Specifically, this incorrect input made the Fe–O–Fe link appear asymmetric when it, in fact, was symmetric. Relevant corrected values now appear in Table III.

(29) Nonlinear parameter estimation and model development program: MINSQ, MicroMath Scientific Software, Salt Lake City, UT 84121.
(30) Dawson, J. W.; Gray, H. B.; Hoenig, H. E.; Rossman, G. R.; Schredder, J. M.; Wang, R.-H. *Biochemistry* **1972**, *11*, 461–465.
(31) Gorun, S. M.; Lippard, S. J. *Inorg. Chem.* **1991**, *30*, 1625–1630 and references therein.

from 50 mV/s up to 800 mV/s). The relative intensities of the peaks suggest complex **2** is reduced by two independent reduction processes, each involving the same number of electrons. While further studies are necessary and ongoing to elucidate the nature of the reduced chemical species, a comparison of the voltammogram of **2** to that of **1** clearly indicates that the glutarate ligand does, indeed, provide additional stabilization to the tetranuclear complex.

Conclusion

We have synthesized a novel Hr-model complex in which two $[Fe_2O(O_2CR)_2]^{2+}$ cores are linked by both the capping ligand L and the dicarboxylate glutarate. The resulting tetrameric cage complex, **2**, has been shown to be spectroscopically, magnetically, and structurally nearly identical to the monocarboxylate-containing tetrameric complex **1**. Furthermore, both complexes **1** and **2** are accurate model complexes for the essential structural and spectroscopic features of the metazido form of Hr. Despite these similarities, the two complexes have significantly different electrochemistry. The use of the dicarboxylate in **2** to link two $[Fe_2O(O_2CR)]^{2+}$ cores appears to impart additional stability (as compared to the acetate-containing complex **1**) to the "dimer of dimers" or tetrameric Hr-model structure. Analogous behavior has not been observed in simple, dimeric Hr-model complexes that contain a dicarboxylate ligand.[27] As such, this study represents an attractive starting point for the development of Hr-model complexes that, like the protein, can undergo reversible redox chemistry. Furthermore, it indicates that higher order oligomeric iron complexes containing the $[Fe_2O(O_2CR)]^{2+}$ core may not just be of purely intrinsic interest from a structural and synthetic standpoint but may, in fact, prove useful in the development of functional Hr-model compounds.

Acknowledgment. We wish to thank Dr. A. K. Burrell for assistance with the curve-fitting of the magnetic data and in obtaining the electrochemical results. J.L.S. acknowledges the NIH (Grant No. GM 36348), the NSF (PYI Award 1986), and the Camille and Henry Dreyfus Foundation (New Faculty Award, 1984; Teacher-Scholar Award, 1988) for partial funding for this work. J.T.M. thanks the Robert A. Welch Foundation (Grant No. F-1191) for financial support.

Supplementary Material Available: Figures showing a plot of χ_M^{corr} vs T for solid **1** and a view of the unit cell packing diagram and tables of anisotropic thermal parameters for the non-hydrogen atoms, positional and isotropic thermal parameters for the H atoms, and bond lengths and angles (15 pages). Ordering information is given on any current masthead page.